

# Disordered state in first-order phase transitions: Hexagonal-to-cubic and cubic-to-hexagonal transitions in boron nitride

M. I. Eremets\*

*National Institute for Research in Inorganic Materials, Tsukuba, Ibaraki 305, Japan;  
CREST, Japan Science and Technology Corporation (JST), Kawaguchi, Saitama, 332, Japan;  
Institute of Spectroscopy, Academy of Sciences of Russia, Troitsk, Moscow region, 142092, Russia;  
and Center for Superhard Materials, Ministry of Science, 142092, Troitsk, Moscow region, Russia*

K. Takemura, H. Yusa, D. Golberg, and Y. Bando

*National Institute for Research in Inorganic Materials, Tsukuba, Ibaraki 305, Japan*

V. D. Blank

*Institute of Spectroscopy, Academy of Sciences of Russia, Troitsk, Moscow region, 142092, Russia  
and Center for Superhard Materials, Ministry of Science, 142092, Troitsk, Moscow region, Russia*

Y. Sato and K. Watanabe

*National Institute for Research in Inorganic Materials, Tsukuba, Ibaraki 305, Japan*

(Received 10 June 1997; revised manuscript received 31 October 1997)

The microscopic mechanism of diffusion-type solid-solid first-order transitions was studied in boron nitride. This substance exhibits an extreme case of transitions between very different lattices, hexagonal (graphite-like) and cubic (diamond-like) phases, accompanied by a large change in the volume. A boundary between the hexagonal and cubic phases was produced by local heating of either a cBN or hBN sample in a diamond-anvil cell under hydrostatic pressure with the aid of a laser so that the sample was partially transformed to another phase. The boundary was studied with the aid of micro-Raman and high-resolution electron microscopy. In the transient region between the two phases a mixture of highly fragmented disordered nanocrystallites and the amorphous state of BN was found. BN nanotubes growing from the amorphous state were also discovered in this region. [S0163-1829(98)04510-X]

## I. INTRODUCTION

First-order phase transitions cover a lot of phenomena. A general theory has not been constructed and many questions are unclear.<sup>1</sup> An important point is a microscopic picture of the progress of the transition. A common feature of first-order transitions is the coexistence of nuclei of the new phase and the parent phase. The new phase is built through a layer around the nuclei. This layer is believed to be very thin, of the order of a few atomic distances in the vapor-liquid and liquid-solid transitions. The solid-solid transitions, on the other hand, have a specific feature: both the new and parent phases have rigid lattices. These lattices can be of completely different structures in diffusion-type transition with large difference in volume. Because of this volume jump stresses will appear around the nuclei of the new phase, which can lead to the fracturing and fragmentation of the surrounding single-crystal parent phase.<sup>2</sup> It is natural to expect a disordered layer between the new and parent phases. Observation of this layer is however a difficult experimental problem, because it is metastable and exists at the transient stage of the phase transformation. It should be observed *in situ* at the corresponding pressure or temperature.

Boron nitride is suitable for such studies. It has completely different diamondlike cubic (cBN) and graphite-like hexagonal (hBN) phases with an extremely large change of volume ( $\Delta V/V=0.53$ ). Because of this large jump in vol-

ume, fragmentation and disordering of substance between the two phases can develop pronouncedly. In combination with the rigid lattices it leads to the very large hysteresis of the phase transitions and hence the phases created under high-pressure high-temperature conditions can remain in the recovered samples. BN has also metastable rhombohedral and wurtzite phases in addition to the stable hexagonal and cubic modifications. The sequence of the phase transitions between these phases is determined not only by the equilibrium phase diagram, but also by kinetic factors and the starting material.<sup>3,4</sup> In the present study we concentrate on the direct diffusion-type transitions between the equilibrium phases cBN and hBN. To make these transitions dominant the starting materials were chosen as partly disordered hBN for the study of the hBN-cBN transition and single crystalline cBN for the cBN-hBN one.

Figure 1 shows the phase diagram of BN.<sup>5</sup> A feature of the BN phase diagram is the large hysteresis of direct transitions without a catalyst: the lines for direct and back transformations (thick solid lines) strongly deviate from the equilibrium phase boundary (dashed line). To bring cBN to the hBN state (path 1) it is necessary to apply a pressure and, in addition, a temperature to overcome the activation barrier. cBN “graphitizes” only at  $\sim 1500$  K at ambient pressure, and at higher temperatures under elevated pressures.<sup>4,5</sup> The same is valid for the back transformation: the lowest pressure for the direct hBN-cBN transformation is about 8 GPa at the

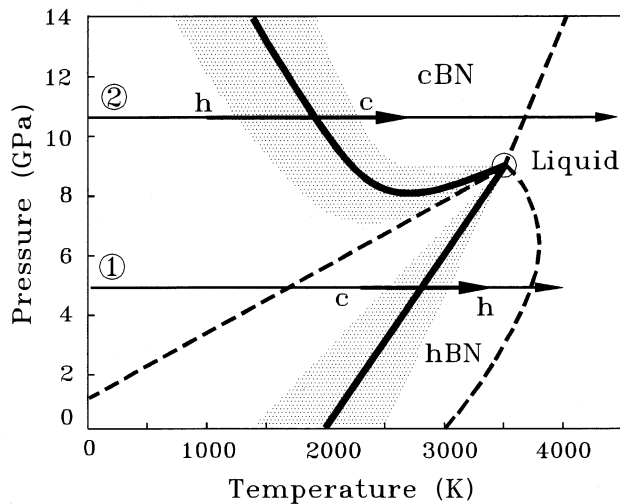


FIG. 1. The pressure-temperature phase diagram of BN. The dashed lines show equilibrium phase boundaries according to Bundy and Wentorf (Ref. 5). The thick solid lines indicate the approximate boundaries for the direct cBN-hBN and hBN-cBN transformations. The hatched area roughly indicates the regions where the transformations are kinetically possible. Horizontal arrows show typical experimental runs at constant pressure, path 1 for cBN to hBN and path 2 for hBN to cBN transformations.

temperature  $\sim 3000$  K, and the transformation pressure increases with decreasing temperature.<sup>3,5</sup> As a result, if a cBN sample is heated under a pressure below  $\sim 8$  GPa (path 1), it transforms to hBN and remains in this state under cooling, because the line of the back transition is not intersected. Similarly, if a hBN sample is heated above 10 GPa (path 2), it irreversibly transforms to the cubic phase.

To study the microscopic mechanism of the solid-solid transformation, a boundary between cBN and hBN was created. To do this, a single phase sample of cBN or hBN was locally heated by a laser in a diamond-anvil cell (DAC). Because of the temperature gradient over the sample a new phase appeared in the heated region separated by a definite boundary from the unchanged cool part of the sample. Under laser heating, all parts of the sample are at the same pressure, but they transform to another phase according to the temperature in the particular place. The transformation “wave” spreads out over the sample under heating. The boundary stops at the line corresponding to the lowest temperature where the transition is still possible at the given pressure. Thus the kinetics of the structural transformations (which would occur with the sample as a whole being placed into uniform temperature field) is spatially recorded over the sample as a “snapshot” of the phase transformation. In the present experiments a mixture of highly fragmented disordered nanocrystals and amorphous BN was found at the boundaries both in the hBN-cBN and cBN-hBN transformations.

## II. EXPERIMENTAL

The sample of hBN (Ref. 6) or cBN (Ref. 7) in the form of a platelet of  $\sim 10 \times 100 \times 100 \mu\text{m}$  was placed in a DAC for pressurization and heating.<sup>8</sup> Pressure was measured by a ruby gauge.<sup>9</sup> Usually, the measured pressure dropped after

heating by about 0–0.8 GPa. We refer to the lower value of the pressure throughout the present study. Nitrogen was loaded into the DAC at low temperature and was used as a pressure medium. It provides ideal hydrostaticity upon heating and prevents dissociation of BN. The BN samples heated in nitrogen did not change the stoichiometry: Raman spectra and x-ray diffraction patterns of the heated samples are characteristic for hBN and cBN. The electron energy-loss spectroscopy (EELS) spectra of the heated samples show the B to N ratio close to 1. On the other hand, if we use Ar as a high-pressure medium, it incorporates into the BN samples after heating.<sup>10</sup> The  $10.6 \mu\text{m}$  CO<sub>2</sub>-laser radiation is directly absorbed by optical phonons in cBN and through two-phonon processes in hBN. The cw CO<sub>2</sub>-laser radiation ( $\sim 100$ W) was focused to a spot of diameter  $80 \mu\text{m}$  at the edge of the sample. The sample was heated over 1 min while increasing the laser power until it shone brightly and changed the shape. After that, the laser radiation was quickly shut off in less than 1 s.

Temperature was not measured in the present study. We estimate the maximum temperature achieved to be above 3290 K (the melting temperature of hBN at a nitrogen pressure of 50 MPa [Ref. 11]), because traces of local melting were observed at the edges of the heated area. At the periphery of the laser spot the sample was nearly unheated and remained unchanged. Thus the sample was subjected to a large temperature gradient.

The recovered samples were studied with micro-Raman spectroscopy and high-resolution transmission electron microscopy (HRTEM). Micro-Raman measurements were done with a triple spectrometer Jasco NR-1800 with a  $100\times$  objective, which focuses a laser beam to a spot of  $\sim 1 \mu\text{m}$ . The micro-Raman scanning over the sample gives information about the evolution of the phase transformation, however, the local picture below the submicron scale is potentially averaged over both crystalline and amorphous states. The points of interest were then analyzed on the atomic scale with the HRTEM. A field-emission-type electron microscope JEOL 3000F was used operating at 300 kV equipped with apparatuses for energy-dispersive x-ray and EELS analysis. High-resolution images were obtained with  $4 \times 10^5$  times magnification.

## III. EXPERIMENTAL RESULTS

### A. Transformation from cubic to hexagonal phase

Cubic BN single-crystal samples were heated at high pressures ranging from 5.1 to 7.7 GPa. They always kink at the boundary between the heated and unheated area (Fig. 2), probably because of the large change of volume during the cBN-hBN transition. The remainder of the platelet shows an unchanged cubic single-crystal phase. The transformed part of the sample was examined at atmospheric pressure with the angle-dispersive powder x-ray-diffraction technique by using a  $40 \mu\text{m}$  diameter beam from the synchrotron radiation source at the Photon Factory, Japan. A diffraction pattern of a perfect polycrystal of hBN was obtained. The samples were carefully scanned with micro-Raman. At the coolest and hottest edges of the sample typical spectra for cubic and hexagonal phases were recorded [Fig. 2(b)]. In the transient region from cBN to hBN the large increase of luminescence

## cBN $\Rightarrow$ hBN

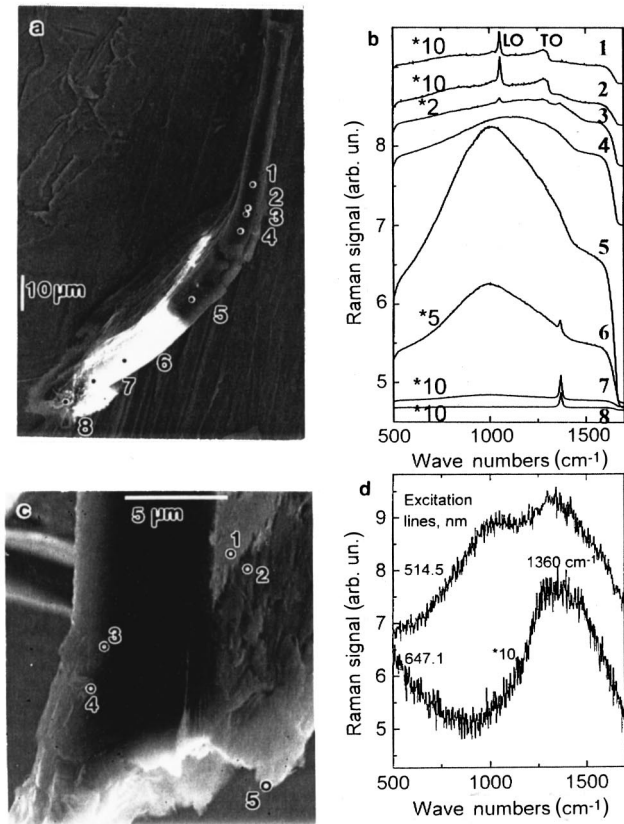


FIG. 2. Micro-Raman scanning of the transient region between cBN and hBN parts of the initially single crystal cBN sample. (a) A SEM view of the cBN sample recovered after laser heating at 6.0 GPa. The lower half of the sample was heated, which looks bright in the photograph. The boundary between heated and unheated area is located around points 3 and 4. The initially platelet-form sample kinked after heating. (b) Raman spectra recorded from the marked points in (a). (c) The cBN sample heated at 5.1 GPa. This is a piece split from the whole sample at the boundary between the heated and unheated parts. Micro-Raman probes are marked on the surface (points 1 and 2) and inside (split plane, points 3 and 4). The recorded spectra are similar to ones shown in (b) (spectra number 2–5). (d) Raman spectra recorded at the split edge similar to point 5 in (c). Different wavelengths of the laser excitation were used as indicated.

obscures the Raman spectra. The luminescence sharply increases by more than two orders of magnitude within a  $2 \mu\text{m}$  scan just at the edge of the cubic phase and the transient region [points 1 and 2 in Fig. 2(c)]. This was observed for all cBN samples examined with micro-Raman after heating. This is not an effect of surface contamination: the same was observed during scanning of a split plane, i.e., inside the sample [points 3 and 4 in Fig. 2(c)]. The luminescence was partly eliminated with the aid of red excitation lines [Fig. 2(d)]. A broad Raman peak with width of  $\approx 400 \text{ cm}^{-1}$  developed.

The transient region between the phases was examined also with HRTEM. The heated samples were split in a similar way as shown in Fig. 2(c), and a piece was placed onto a carbon grid for HRTEM. The sharp transparent edges of the samples [similar to point 5 in Fig. 2(c)] were examined. A

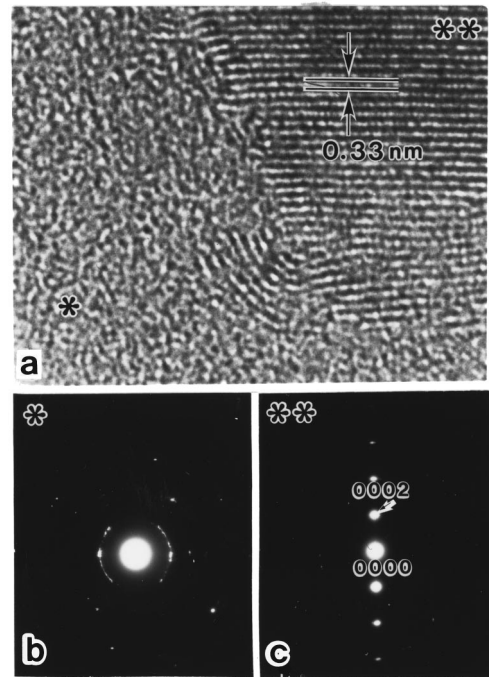


FIG. 3. HRTEM data for the transient region between cBN and hBN parts for the cBN sample heated at 5.1 GPa. (a) A HRTEM view of the transparent sharp edge of the sample similar to the point 5 in Fig. 2(c). A mixture of amorphous and turbostratic hBN is typical. The interlayer distance of 0.33 nm in the turbostratic region is in agreement with hBN. (b, c) Corresponding electron-diffraction patterns from the marked points in (a).

mixture of apparently disordered structure and small crystals of the hexagonal phase is typical for this region (Fig. 3).

### B. Transformation from hexagonal to cubic phase

A platelet of hBN ( $\sim 10 \times 100 \times 100 \mu\text{m}$ ) was split from a tablet of the pyrolytic BN. The hBN sample was heated at 10.1 GPa. Figure 4(a) shows a SEM view of the recovered sample, in which the laser radiation was focused to three points A, B, and C. The starting material looks dark, while the transformed material is light. The shape of the sample did not change significantly. Traces of melting were observed only at the edges of the points A, B, and C. Because of the low thermal conductivity of the hBN polycrystal the sample was not melted through [Fig. 4(b)].

To study the transient region between the hexagonal and cubic parts, the sample was split [Fig. 4(c)] so that the interior of the sample could be scanned with a micro-Raman probe. A surface scan was also done, which generally agreed with the interior one. A series of Raman spectra is shown in Fig. 4(d). At a distance of  $\approx 20 \mu\text{m}$  Raman spectra change from the typical spectrum of the partly disordered starting hBN to the perfect spectrum of the cubic phase. The region between the two phases is not a simple mixture of cubic and hexagonal phases: (a) the  $1365 \text{ cm}^{-1}$  line is abruptly broadened and shifts to  $1358 \text{ cm}^{-1}$ . The width is  $200\text{--}300 \text{ cm}^{-1}$  for all points in the transient zone. (b) A broad line appears at  $750 \text{ cm}^{-1}$  simultaneously with the broad  $1358 \text{ cm}^{-1}$  line.

HRTEM data showed a partly turbostratic structure for the starting hBN sample, a highly disordered phase mixed

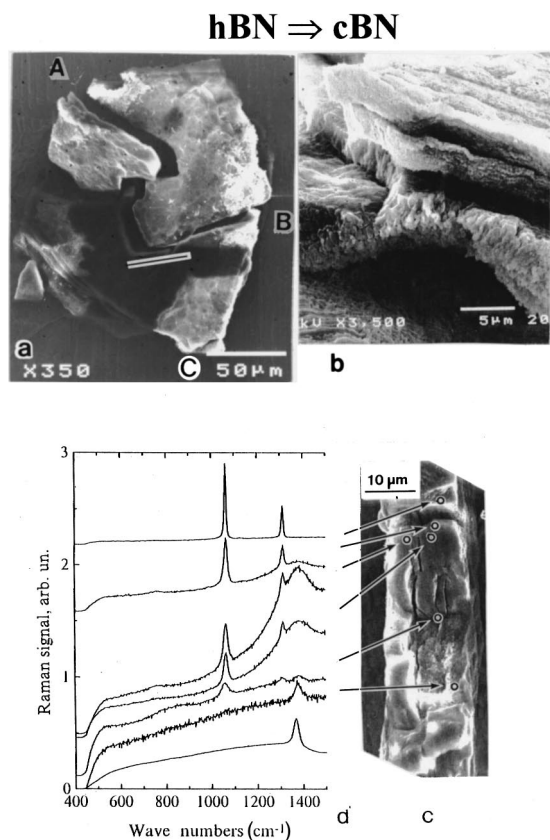


FIG. 4. Micro-Raman scanning over a boundary between the starting hBN polycrystalline part of the sample and the cBN one created after the laser heating. (a) A SEM view of the recovered sample heated at regions A, B, and C at the pressure of 10.1 GPa. The lower split part of the sample was used for micro-Raman scanning. (b) An enlarged side view of the sample in the region A. Traces of melting can be seen at the bottom where the sample was irradiated. (c) A cross section of the sample at the straight line in (a). The upper half of the sample was heated. (d) The Raman spectra from the corresponding points in (c). The Raman signal probes a volume of diameter less than  $2 \mu\text{m}$  and  $\sim 1 \mu\text{m}$  depth. The Raman spectra change from typical ones for hBN (bottom) to those for cBN (top). The bottom spectrum was recorded from a point which lies below the margin of the view, in the unheated part.

with a turbostratic phase in the transient region [Fig. 5(a)], and a highly crystalline cubic phase with numerous twins in the cBN region [Fig. 5(b)].

### C. BN nanotubes

Unexpectedly, BN nanotubes were found in the transient regions between the two phases both in the hBN-cBN and cBN-hBN transformations (Fig. 6).<sup>12</sup> The nanotubes grew from the disordered material. We found that the basement for this amorphous layer is either cBN or hBN.

## IV. DISCUSSION

Our results give clear evidence for the existence of an amorphous (or disordered) material together with nanocrystals in the transient region both for cBN-hBN and hBN-cBN transitions. First, it follows from direct atomic-scale observations with HRTEM that the structure is apparently disor-

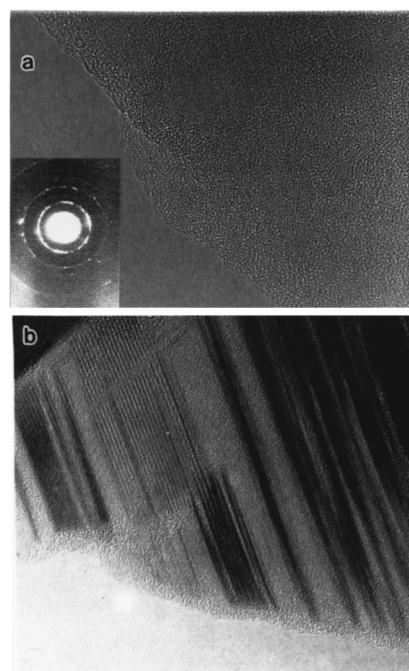


FIG. 5. HRTEM views of the hBN sample laser heated at 10.1 GPa. (a) Typical view of the transient region between hBN and cBN parts of the sample. The inset is the electron-diffraction pattern from the area approximately corresponding to the whole image. (b) cBN crystallites from the transformed part of the sample.

dered. However, traces of crystallinity remain in the electron-diffraction patterns [Figs. 3(b) and 5(a)]. EELS spectra taken from the disordered region in Fig. 3 show hexagonal B-N bonding. These data are therefore not sufficient to show whether the region consists of a mixture of the true

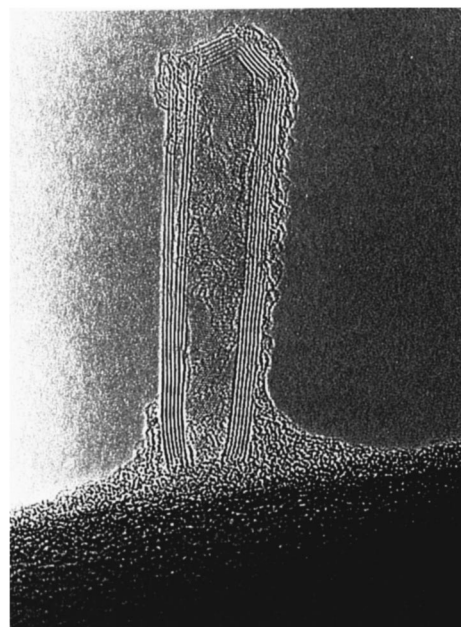


FIG. 6. A BN nanotube found in the transient region between the hBN and cBN parts of the hBN sample, which was laser heated at 10.1 GPa as shown in Fig. 4. The distance between layers of the tube wall is about 0.33 nm.

amorphous state and nanocrystals, or the amorphous state still contains a short-range ordering.

Micro-Raman scanning measurements also show the existence of a disordered state in the transient region. The broadening of the  $1365\text{ cm}^{-1}$  Raman peak (Figs. 2 and 4) is a characteristic feature. This broadening cannot be explained simply by the decrease in size of the hBN crystallites. A correlation has previously been observed between the size of hBN crystallites and the width of their Raman peaks.<sup>13</sup> Extrapolation to the present broadening of  $250\text{ cm}^{-1}$  gives a crystallite size of  $\sim 0.6\text{ nm}$ . This is not a realistic value. We suppose that the broad spectra are not due to the size effect of crystallites but represent an amorphous state. An inherent feature of Raman spectra of amorphous solids is a gap in the correlation length between amorphous and crystalline states: the lowest limit is  $1.2\text{--}1.5\text{ nm}$  for Si.<sup>14</sup> Consequently, the Raman spectrum of amorphous Si is very broad ( $\sim 200\text{ cm}^{-1}$ ) while microcrystals of Si give a width of the Raman line  $< 40\text{ cm}^{-1}$  even for the crystal dimension of  $4\text{ nm}$ . Raman spectra of amorphous BN are unknown.<sup>15</sup> We notice that the recorded Raman spectra in the transient region are very similar to those of the analogous material, amorphous carbon.<sup>14,16</sup>

Another feature of the Raman spectrum of BN is the appearance of additional peaks around  $750\text{ cm}^{-1}$  and the shift of the  $1365\text{ cm}^{-1}$  peak to lower energies in addition to its broadening. This can be explained by relaxation of the selection rules in amorphous materials: most phonon modes become Raman active so the Raman spectrum reflects mainly the density of states of phonons. In particular, the out-of-plane  $w_{13} = 783\text{ cm}^{-1}$ ,  $w_{13} = 828\text{ cm}^{-1}$  modes (normally only infrared active<sup>17</sup>) can develop in the Raman spectrum.

The amorphous state is also clearly evidenced by the observation of the BN nanotubes. We have found nanotubes in three different cases: in the transient region during cBN-hBN transition, hBN-cBN transition, and in BN microcrystals grown from a fluid at  $\approx 8\text{ GPa}$ , around the triple point of BN.<sup>8</sup> The nanotubes apparently grow from the amorphous state on the surface of the crystals (Fig. 6). In all these cases the substance is in the region of instability between two (hBN and cBN) or three (hBN, cBN, and liquid) phases. The finding of nanotubes is an indirect but strong evidence of the existence of the amorphous state in the hBN-cBN and cBN-hBN transformations.

We suppose that the observed disordered state is inherently related to the direct transformations between cBN and hBN. An alternative explanation is its creation from BN crystalline phases by rapid cooling. However, it seems unlikely because the disordered state was *only* observed at the boundary between the two phases, where temperatures are the minimum needed to initiate the transformations. Cooling from these temperatures most probably cannot change the rigid lattices of BN phases, especially at high cooling rates. Amorphous BN can also be produced by chemical reactions.<sup>15,18</sup> It converts irreversibly to hBN at temperatures  $\approx 1400\text{ K}$ .<sup>15</sup> This fact indirectly supports the idea that the amorphous state was formed at high temperature and quenched during rapid cooling. Otherwise, under slow cooling it can transform to the crystalline phases.

Another possibility of the appearance of the amorphous state is the amorphization of the high-pressure phase during

decompression at low temperatures. It was observed, for example, in some III-V compounds.<sup>19</sup> In these cases the amorphous phase transforms to a low-pressure crystalline phase upon heating at atmospheric pressure. However, this is not the case of BN: cBN is stable over a large  $P$ - $T$  domain (Fig. 1), in particular, at low pressures and temperatures. cBN is stable during decompression even from the pressure of  $115\text{ GPa}$  at room temperatures.<sup>20</sup>

Fragmentation of the starting material was observed with HRTEM at some stages of the phase transformations (Fig. 5). The fragmentation is accompanied by the creation of dangling bonds and other defects. Their formation can explain the enhanced luminescence appearing just at the beginning of the phase transformation in the single crystal (Fig. 2). The enhanced concentration of defects around the growing phase is important for understanding the growth process limited by self-diffusion. To build a new crystal the atoms have to have high mobility along the boundary of the growing crystal. The existence of an amorphous state with numerous defects can drastically increase the self-diffusion coefficient  $D \sim \exp(-zE/k_B T)$ . If the activation energy  $E$ , which is estimated to be about  $5\text{ eV}$  from the value for diamond, changes by  $20\%$ , the diffusion coefficient  $D$  will change by two orders of magnitude.

Fragmentation of a starting single crystal down to nanoscale domains was observed during first-order phase transitions.<sup>21-23</sup> Amorphization under pressure has also been found in a number of solids.<sup>24-27</sup> We think that both phenomena, the fragmentation and the amorphization under pressure, are related to the present study and are the consequence of the microscopic mechanism of the solid-solid first-order transition. The following model can be proposed. Numerous nuclei of the new phase grow with pressure, causing fracturing and fragmentation of the parent phase. An amorphous layer appears around the nuclei of the new phase. Through this layer, atoms from the surrounding parent phase diffuse to build the new phase. To do this in solid, it is necessary to provide the atoms with a high mobility along the growth boundary. Atomic layers at the growth boundary have to be disordered with a high concentration of vacancies and defects. The amount of layers depends on the material and the stage of the transformation. Importantly, since its volume is proportional to the surface area of the nuclei of the new phase, the total volume of the amorphous state has a maximum at a certain stage of the phase transformation. The amorphous state decreases with the growth of the crystals of the new phase and disappears upon full transformation. The amorphous layer is a metastable state and usually recrystallizes upon release of pressure. In some materials, as in the present case of BN, this metastable state remains and can be studied in the recovered samples.

It is natural to suppose that the amorphous state is common in first-order diffusion-type phase transitions and exists at the boundary between strongly different crystal lattices. However, in the majority of cases such a state is difficult to detect for several reasons: it may be of extremely small quantity and produce a very weak and broad x-ray-diffraction pattern or Raman spectrum; it is metastable and recrystallizes, and therefore has to be studied *in situ* or in the materials with large hysteresis. BN and carbon are attractive materials for studying first-order transitions. Both the large

change in the lattices during the transition and their hysteresis allow the detailed study of the lattice structure in atomic resolution in the recovered samples.

## V. CONCLUSIONS

The phase boundary at the first-order phase transition was studied in the cubic-to-hexagonal and hexagonal-to-cubic transitions in BN. The starting cubic or hexagonal samples were partially transformed into another phase and the transient region between the two phases was studied. A mixture of a disordered material and nanocrystallites is typical for this region. We suppose that this is a general feature of the progress of the solid-solid reconstructive (diffusion-type) first-order transitions: the growth of a new phase is accom-

panied by the fragmentation of the parent crystal and the creation of a disordered amorphous layer between crystallites of the parent and new phases. This layer is saturated with defects, and atoms diffuse from one lattice to the other one with a high mobility.

## ACKNOWLEDGMENTS

M.I.E and D.G. are grateful for the grant from NIRIM, Tsukuba, Japan, where the experimental part of this work was done. We are grateful to N. N. Melnik for the Raman experiment, G. A. Dubitskii for supplying us with the cubic BN samples, V.V. Aksenkov for the x-ray measurements, O. A. Louchev for helpful discussions, and J. Hester for checking the manuscript.

- 
- \*Author to whom correspondence should be addressed. Present address: Research Center for Materials Science at Extreme Conditions, Osaka University, Osaka 560, Japan.
- <sup>1</sup>J. D. Gunton, M. San Miguel, and P. S. Sahini, in *Phase Transitions and Critical Phenomena*, edited by C. Domb and J. L. Lebowitz (Academic, London, 1983), Vol. 8.
  - <sup>2</sup>P. Gillet, Y. Gerard, and C. Willaime, *Bull. Mineral.* **110**, 481 (1987).
  - <sup>3</sup>N. I. Bornichuk *et al.*, *Sov. Phys. Dokl.* **306**, 1381 (1989).
  - <sup>4</sup>A. V. Kurdyumov, I. S. Gladkaya, A. S. Golubev, G. A. Dubitskii, V. N. Slesarev, G. S. Olejnik, and N. F. Ostrovskaya, *Inorg. Mater.* **18**, 1835 (1982).
  - <sup>5</sup>F. P. Bundy and R. H. Wentorf, Jr., *J. Chem. Phys.* **38**, 1144 (1963); F. R. Corrigan and F. P. Bundy, *ibid.* **63**, 3812 (1975). An alternative phase diagram was proposed by V. L. Solozhenko, *J. Hard Mater.* **6**, 51 (1995). The difference between these diagrams does not alter the interpretation of our data, and we refer to the first diagram.
  - <sup>6</sup>A. V. Kurdyumov, *Sov. Phys. Crystallogr.* **20**, 969 (1975). We used pyrolytic hBN having a three-dimensional ordering parameter  $P_3=0.5$ , where  $P_3=N_3/N$ .  $N_3$  is the number of layers which are oriented regularly with respect to the nearest layers, and  $N$  is the total number of layers in the coherent scattering region. The average size of crystal grains was 6–10 nm, deduced from the broadening of the x-ray diffraction peaks and direct HRTEM observations. The sample contains a negligible amount of the rhombohedral phase judging from the x-ray and Raman spectra.
  - <sup>7</sup>I. S. Gladkaya, G. A. Dubitskii, and V. N. Slesarev, *Acta Crystallogr., Sect. A: Cryst. Phys., Diffr., Theor. Gen. Crystallogr.* **34**, S214 (1978). The platelets of cBN of thicknesses less than 10  $\mu\text{m}$  were synthesized in a BN-LiH system under pressure.
  - <sup>8</sup>M. I. Eremets, K. Takemura, H. Yusa, D. Golberg, Y. Bando, and K. Kurashima, in *Advanced Materials '96*, edited by M. Akaishi *et al.* (International Communications Specialists, Tokyo, 1996), p. 169.
  - <sup>9</sup>H. K. Mao, P. M. Bell, J. W. Shaner, and D. J. Steinberg, *J. Appl. Phys.* **49**, 3276 (1978).
  - <sup>10</sup>D. Golberg, Y. Bando, M. Eremets, K. Kurashima, T. Tamiya, K. Takemura, and H. Yusa, *J. Electron Microsc.* **46**, 281 (1997).
  - <sup>11</sup>V. L. Vinogradov and A. V. Kostanovski, *Teplotiz. Vys. Temp.* **29**, 1112 (1991).
  - <sup>12</sup>D. Golberg, Y. Bando, M. Eremets, K. Takemura, K. Kurashima, and H. Yusa, *Appl. Phys. Lett.* **69**, 2045 (1996).
  - <sup>13</sup>R. J. Nemanich, S. A. Solin, and R. M. Martin, *Phys. Rev. B* **23**, 6348 (1981).
  - <sup>14</sup>M. H. Brodsky, *Light Scattering in Solids I* (Springer, Berlin, 1983), p. 205.
  - <sup>15</sup>H. Sumiya, T. Iseki, and A. Onodera, *Mater. Res. Bull.* **18**, 1203 (1983).
  - <sup>16</sup>Q. Wang, D. D. Allerd, and J. Gonzalez-Hernandez, *Phys. Rev. B* **47**, 6119 (1993).
  - <sup>17</sup>R. Geick, C. H. Perry, and G. Ruprecht, *Phys. Rev.* **146**, 543 (1966).
  - <sup>18</sup>E. J. M. Hamilton, S. E. Dolan, C. M. Mann, H. O. Colijn, C. A. McDonald, and S. G. Shore, *Science* **260**, 659 (1993).
  - <sup>19</sup>K. Tsuji, Y. Yamamoto, Y. Katayama, and N. Koyama, in *High Pressure Science and Technology — 1993*, edited by S. C. Schmidt, J. W. Shaner, G. A. Samara, and M. Ross (AIP, New York, 1994), p. 311.
  - <sup>20</sup>E. Knittle, R. Wentzcovitch, R. Jeanloz, and M. L. Cohen, *Nature (London)* **337**, 349 (1989).
  - <sup>21</sup>J. M. Besson, J. P. Itié, A. Polian, and G. Weill, *Phys. Rev. B* **44**, 4214 (1991).
  - <sup>22</sup>U. D. Venkateswaran, L. J. Cui, and B. A. Weinstein, *Phys. Rev. B* **45**, 9237 (1992).
  - <sup>23</sup>M. Kobayashi, H. Iwata, T. Horiguchi, and S. Endo, *Phys. Status Solidi B* **198**, 521 (1996).
  - <sup>24</sup>M. Kruger and C. Meade, *Phys. Rev. B* **55**, 1 (1997), and references therein; E. G. Ponyatovsky and O. I. Barcalov, *Mater. Sci. Rep.* **8**, 147 (1992).
  - <sup>25</sup>O. Mishima, L. D. Calvert, and E. Whalley, *Nature (London)* **310**, 393 (1984).
  - <sup>26</sup>M. Kruger and R. Jeanloz, *Science* **249**, 647 (1990).
  - <sup>27</sup>P. Gillet, J. Badro, B. Varrel, and P. F. McMillan, *Phys. Rev. B* **51**, 11 262 (1995).